9-15-2000

Resolving Ambiguities in Gravity Wave Propagation Directions Inherent in Satellite Observations: A Simulation Study

Michael P. Hickey Ph.D.
Embry-Riddle Aeronautical University, hicke0b5@erau.edu

Jason S. Brown
Clemson University

GEOPHYSICAL RESEARCH LETTERS, VOL. 27, NO. 18, PAGES 2901-2904, SEPTEMBER 15, 2000

Resolving Ambiguities in Gravity Wave Propagation Directions Inherent in Satellite Observations: A Simulation Study.

Michael P. Hickey and Jason S. Brown

Department of Physics and Astronomy, Clemson University, Clemson SC 29634-0978

Abstract. We simulate space-based, sub-limb viewing observations of airglow brightness fluctuations caused by atmospheric gravity wave interactions with the O_2 atmospheric airglow, and we demonstrate that, due to the geometry associated with such observations, the brightness fluctuations observed for the optically thick 0-0 band emission will always appear stronger for waves traveling towards the observer (satellite). The effect should be most noticeable for waves having relatively small vertical wavelengths (~ 10 km) and horizontal wavelengths of 50 km or greater. For waves of short (~ 100 km) horizontal wavelength, the brightness fluctuation anisotropy with respect to viewing direction may also be evident in the optically thin 0-1 band emission. Therefore, the 180° ambiguity in wave propagation direction associated with space-based observations may be eliminated for waves dissipating in the upper mesosphere and lower thermosphere.

1. Introduction

It has become clear that in order to improve our understanding of the influences of atmospheric gravity waves on the mesosphere/lower thermosphere (MLT) region momentum and energy budgets, global characterization of the waves acquired through long-term, global observations using one or more suitably instrumented satellites is required. Because typical satellite orbital speeds (~ 8 km/s) greatly exceed typical MLT region gravity wave phase speeds (≤ 100 m/s), the wave system appears stationary to satellites. Therefore, even when the orientation of the phase fronts with respect to azimuth can be determined from such observations, there exists a 180° ambiguity in the inferred direction of wave propagation. Resolving this ambiguity is critical to the determination of gravity wave momentum forcing of the mean state.

This ambiguity in propagation direction can be eliminated by combining coincident ground-based observations with satellite observations, however, such an approach has obvious limitations. First, the geographical distribution of the limited number of suitable ground stations is not well suited for such correlative studies. Two-thirds of the ocean-covered Earth is not accessible to such sites, which would bias the inferred wave spectra (e.g., *Fritts et al.*, 1989). Second, ground-based optical observations are limited by viewing conditions (note that radar observations do not suffer from this limitation). Therefore, it would be highly desirable to develop a method of removing the directional ambiguity using the satellite data alone.

The objective of this study is to demonstrate that the ambiguity associated with the gravity wave propagation direction can be alleviated for waves that are likely to be important to the energy and momentum budgets of the MLT region. We do so using a gravity wave model and a chemistry/airglow fluctuation model to simulate satellite observations of airglow perturbations due to four different waves. Specifically, we simulate forward viewing observations of gravity waves that exist in the airglow in some region ahead of the spacecraft, and backward viewing observations of the same region of the airglow at some later time.

Paper number 1999GL011331.
0094-8276/00/1999GL011331$05.00

2. Method

We a linear, steady-state full-wave model describing the wave dynamics, and a linear, steady-state chemistry model describing wave-driven airglow fluctuations. These models have been previously used to simulate gravity wave-driven fluctuations of the OI 5577 nightglow [*Hickey et al.*, 1997a, 1998; *Schubert et al.*, 1999] and the O_2 atmospheric (hereafter O_2A) 0-1 band nightglow [*Hickey and Walterscheid*, 1999].

Application of these ground-based simulation models to the simulation of space-based observations of airglow variations is facilitated by calculating the total (mean plus wave perturbation) volumetric emission rate as a function of altitude (z) for some arbitrary horizontal position (x). We therefore write $I(x,z) = \overline{I}(z) + I'(x,z)$, where I represents airglow volumetric emission rate, the overbar denotes the unperturbed mean state, and the prime denotes a linear perturbation about the mean state. Our full-wave/airglow fluctuation model provides $I'(x_0,z)$ at the reference position x_0. Assuming a spherical Earth, a horizontally homogeneous mean state, and also that the wave variations in the horizontal direction are purely harmonic with horizontal wave number k, allows us to determine the volumetric emission rate (VER) at any position as $I(x,z) = \overline{I}(z) + I'(x_0,z)\exp[-ik(x-x_0)]$. Simulation of the airglow brightness then proceeds by integration of this quantity along a specified tangent ray path. Our Cartesian coordinates (x,z) are transformed to spherical coordinates (r,θ) using $r = R_E + z$ and $x = r\theta$ (where R_E is the Earth's radius). The validity of this transformation for gravity wave propagation is supported by the work of *Francis* [1972], who has shown that large scale gravity waves are refracted around the spherical Earth by the effects of gravity gradients. The geometry for such observations is shown in Figure 1.

The dynamical/airglow model is used to simulate spaced-based observations of gravity wave-driven O_2A 0-0 and 0-1 band airglow fluctuations. The model output (VER) is interpolated using a smoothing cubic spline. The upper limit of integration along the line of sight corresponds to an altitude of 130 km, encompassing the relevant airglow region. For each calculation, a 400 point Gauss-Legendre quadrature scheme is used to integrate the VER along the constrained line of sight, which is sufficiently accurate to handle the wide range of wave parameters responsible for driving a given airglow response. The direction of viewing is determined relative to the

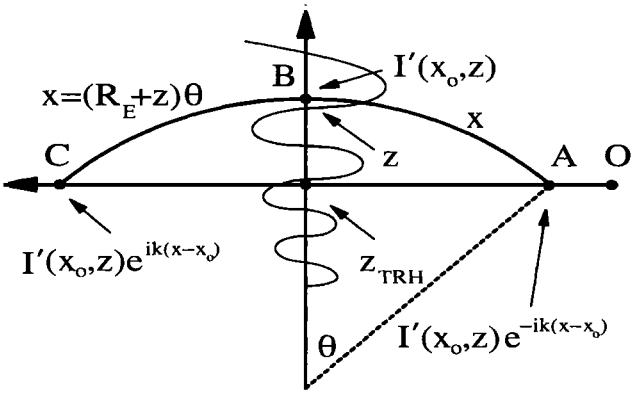

Figure 1. Schematic (not to scale) showing the geometry for wave propagation in a spherical atmosphere as viewed from a satellite. Points A, B, and C all lie at the same altitude, z, and the line of sight (tangent ray path) extends from the observer (at O) through A, C, and the tangent ray point at height z_{TRH}. The arc length, x, and the horizontal wavenumber, k, are used to define the perturbations at A and C in terms of that at B.

direction of motion of the observer. "Forward viewing" ("backward viewing") is defined as viewing along (opposite to) the direction of the observer's motion. The total brightness is calculated as a function of satellite position, and then averaging over three complete wavelengths provides the mean brightness. Half of the difference between these two then provides the brightness perturbation amplitude. A similar procedure could be applied to actual satellite data.

For the optically thick O_2A 0-0 band emission, the self-absorption is calculated using the Lambert-Beer law and a band-averaged optical depth (τ) given by *Wallace and Hunten* [1968], viz., $\tau = 1.6x10^{-22}[O_2](245/T)$, where T is temperature. Values of T and $[O_2]$ are the same as those used in the full-wave model and defined using the MSIS-90 model [*Hedin*, 1991]. These data are also interpolated using a smoothing cubic spline. The amount of absorption is determined at each Gauss-Legendre abscissa, which represents a point along the line of sight. For a given abscissa, the amount of absorption is determined by the integral of the optical depth along the line of sight from this abscissa to the observer. The trapezoidal rule is used for this integration (with an accuracy of ~ four decimal places) and is only implemented between adjacent abscissae to avoid multiple calculations of the same quantities. During final quadrature to obtain the total integrated intensity, each absorption term is multiplied by the value of the VER (the integrand) at a given abscissa, yielding the brightness (for both forward and backward viewing) of the 0-0 band O_2A emission. The mean VER of the O_2A used here peaks at about 91.5 km altitude with a value of 2.76 x 10^8 photons m^{-3} s^{-1}, and has a full-width at half-maximum of about 10 km.

3. Results

We consider four different gravity waves having the parameters given in Table 1. Waves 1 and 2 are fairly slow waves with phase speeds of 30 m s^{-1} and fairly short vertical wavelengths (~ 10 km) at the altitude of the peak O_2A VER. Waves 3 and 4 are faster waves, having phase speeds of about 111 m s^{-1} and 151 m s^{-1} and vertical wavelengths of about 40 km and 61 km, respectively. With fairly modest values of eddy diffusion used in our model (peak values of about 200 m^2 s^{-1} at 90 km altitude) and with the additional effects of molecular diffusion, these waves achieve maximum amplitudes at different altitudes (designated z_{peak}), as provided in Table 1. The actual values of amplitude we used for waves 1 and 2 were based on the requirement that the minimum gradient of total potential temperature be zero [*Orlanski and Bryan*, 1969]. However, for waves 3 and 4, which achieve maximum amplitudes well into the thermosphere, this procedure produced unrealistically large wave amplitudes. So instead, for waves 3 and 4, we set maximum temperature amplitudes equal to 10% of the mean at z_{peak} to ensure that these waves have linear amplitudes everywhere. Consequently waves 3 and 4 have significantly smaller amplitudes than those of waves 1 and 2 within the airglow region (by a factor of between about 5 and 10).

We consider space-based observations using a tangent ray height (z_{TRH}) of 40 km. For the optically thin emission, the airglow emission from the far side of the tangent ray point will make a significant contribution to the observed mean brightness. However, for z_{TRH} =40 km, this "far" region will be lie at a significant distance from the foreground region (~1600km). Therefore, in the case of the short (100 km) horizontal wavelength waves considered, it would be unlikely that a given gravity wave would exist simultaneously at both locations. This is because gravity waves are primarily a local phenomenon, and correlation distances are not usually as large as ~ 16 wavelengths. (Ducted waves are a different matter, but these are not considered here.) Accordingly, we consider only the contribution of the foreground emission when calculating the brightness fluctuations for the optically thick and thin emissions and for the 100 km horizontal waves. We include the contributions from both regions (foreground and background) when we calculate the mean brightness, and also when we calculate brightness fluctuations for the 1000 km horizontal wavelength waves. Note that for z_{TRH} = 40 km and for the optically thick emission, we have found that the VER originating from the far side of the tangent ray point does not contribute to the observed brightness.

Figure 2 is a schematic showing the tangent ray paths (dashed-dotted line), and the slope (at angle ϕ) of gravity wave phase fronts (solid lines) in a spherical atmosphere with respect to the local vertical coordinate (short dashed lines). The satellite initially observes an airglow disturbance at time t while forward viewing, and later at time $t+\delta t$ observes the same airglow disturbance while backward viewing. The apparent wavelengths as seen along the line of sight at the two observing times are represented by the line segments $\overline{AB}$ and $\overline{CD}$, respectively. In general, the apparent wavelengths for forward and backward viewing are not equal. This is a geometry effect, and it arises for wave propagation on a spherical Earth because the phase fronts for waves of short vertical wavelength (such as waves 1 and 2) have a significant tilt from the vertical. The apparent wavelength will always be greater when viewing waves propagating towards the observer (in our case $\overline{CD} > \overline{AB}$). For waves of large vertical wavelength (for which $\phi \approx 0$) the importance of this geometry effect diminishes because the phase fronts for such waves are almost vertical and the perturbation VER is therefore approximately symmetric with respect to viewing direction.

Table 1. Wave parameters used in the simulations.

	Wave 1	Wave 2	Wave 3	Wave 4
λ_x (km)	100	1000	100	1000
λ_z (km)	9.3	9.9	39.6	60.9
T (minutes)	55.6	550	15	110
z_{peak} (km)	120	100	170	140
T'_{peak} (K)	27	14	50	41

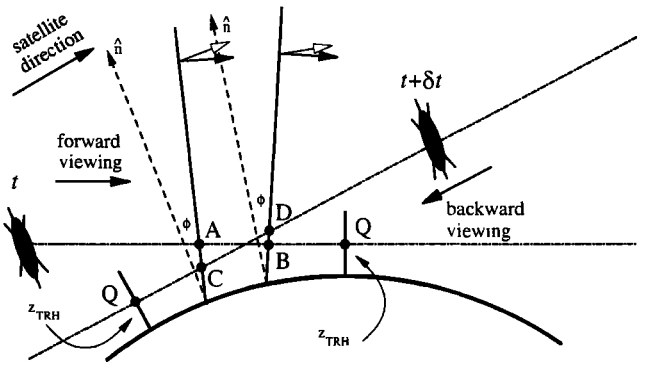

Figure 2. Schematic (not to scale) representing the difference associated with viewing direction of an airglow disturbance. The solid lines represent lines of constant phase at angle ϕ relative to a local vertical coordinate (dashed lines). Arrows represent the total (filled) and horizontal (open) wavenumber vectors. The dashed-dotted lines represent the tangent ray paths for forward (at time t) and backward (at time $t+\delta t$) viewing for a given tangent ray height z_{TRH}. The apparent wavelengths represented by the distances AB (for forward viewing) and CD (backward viewing) are not equal ($CD > AB$), leading to increased destructive interference and a smaller brightness fluctuation for forward viewing.

Figure 3 shows the perturbation VER plotted as a function of distance along the tangent ray from the tangent ray point for wave 1. These results were obtained assuming that the waves and satellite are moving in the same direction. The mean VER (not shown) is symmetrical about the tangent ray point (x=0), but the perturbation VER is not. The apparent wavelength is much smaller for forward viewing (solid curve) than for backward viewing (dashed curve).

Integration of the total VER along the tangent ray provides the observed brightness ($\bar{B}+B'$), where $\bar{B}$ and B' are the undisturbed and perturbation brightness, respectively. Because the apparent wavelength is smaller for forward viewing (as previously noted), the integration leads to smaller brightness fluctuations in this direction as a result of the increased effects of destructive interference. Values of $B'/\bar{B}$ for both forward and backward viewing are presented for the four waves in Table 2. Note that for z_{TRH} = 40 km, $\bar{B}$ is about 4.09

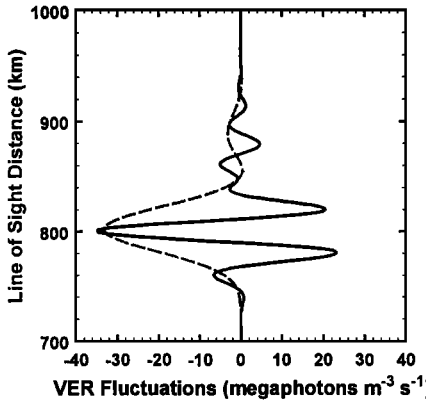

Figure 3. The perturbation volume emission rate (VER) plotted as a function of distance from the tangent ray point along the tangent ray for wave 1. For forward viewing (solid curve) the apparent wavelength is shorter than for backward viewing (dashed curve).

Table 2. Relative brightness fluctuation amplitude for the 0-0 and 0-1 band emissions, for forward and backward viewing, and for the waves described in Table 1.

Wave #	$B'/\bar{B}$ (thin backward)	$B'/\bar{B}$ (thin forward)	$B'/\bar{B}$ (thick backward)	$B'/\bar{B}$ (thick forward)
1	0.055	4×10^{-4}	0.109	5.9×10^{-4}
2	0.035	0.035	0.119	0.070
3	4.9×10^{-3}	1.8×10^{-3}	9.9×10^{-3}	3.6×10^{-3}
4	0.013	0.013	0.025	0.027

x 10^4 R and 2.02 x 10^4 R for the optically thin and optically thick emissions, respectively.

For wave 1, $B'/\bar{B}$ for both the 0-0 and 0-1 band emissions is significantly greater for backward viewing compared to forward viewing. In fact, for forward viewing the waves would be unobservable because the effective wavelength of the wave (along the tangent ray) is very small for this viewing direction (see Figure 3). For backward viewing, $B'/\bar{B}$ is about 11% and 5.5% for the 0-0 and 0-1 bands, respectively. For wave 2 and for the optically thick 0-0 band emission, $B'/\bar{B}$ for backward viewing (~ 12%) exceeds that for forward viewing by a factor of about 1.7. Such differences should be clearly observable. The optically thin 0-1 band emission shows no difference between forward and backward viewing.

For wave 3 $B'/\bar{B}$ is greater for backward viewing than for forward viewing by a factor of about 2.7. Although this is a significant difference, the actual magnitude of $B'/\bar{B}$ is small (less than 1%) and the waves would be unobservable. For wave 4 and for each of the 0-0 and 0-1 band emissions, $B'/\bar{B}$ is essentially the same for both forward and backward viewing. Additionally, the wave amplitudes are quite small (~ 1% – 2%), and the waves would be barely detectable.

4. Discussion

We have employed the band-averaged optical depth (τ) given by *Wallace and Hunten* [1968]. Although our results would be affected by the use of different values of τ (such as those specific to the lines of a particular band being observed), the similarity in results obtained for the optically thin and optically thick emissions (provided in Table 2) suggest that the effect would not be significant.

We have presented nominal results for z_{TRH} = 40 km. Increasing z_{TRH} has the effect of significantly reducing $B'/\bar{B}$ over the nominal values for the λ_x = 100 km waves (for example), implying that the waves would be difficult to observe. For z_{TRH} = 85 km, the number of oscillations in B along the tangent ray significantly exceeds the number associated with z_{TRH}=40 km, leading to increased cancellation effects and to decreased $B'/\bar{B}$ values. A thorough analysis of such effects is presented by *Brown and Hickey* [2000].

Nonlinear effects associated with the small scale-heights of the minor species involved in the airglow emission chemistry may be important for some gravity waves. We have performed calculations using a 2-D, time-dependent, nonlinear model [*Hickey et al.*, 1997b] describing the interactions of gravity waves with the O_2A airglow which confirm the results and conclusions presented here. This demonstrates that our results are not a consequence of nonlinear effects, but instead are due to the geometry effects discussed earlier.

A consideration when viewing the same wave, existing in a given localized region, in the forward and backward viewing

directions is the time delay between such observations. If it is too large, the characteristics of the wave may have changed enough to render the comparison meaningless. For a satellite height of 500 km, z_{TRH} = 40 km, and an orbital period of 100 minutes, the time delay for observing the same volume element of the atmosphere for forward and backward viewing is ~ 7 minutes. This is not large compared to typical internal gravity wave periods (~ 10 to 20 minutes or greater), so that it is reasonable to assume that the wave properties would not change significantly over this time interval.

We have not included height dependent background winds in our analysis. Their effect will be to increase or decrease the local vertical wavelength over its windless value, depending on the direction of wave propagation with respect to the winds, thus affecting the local tilt of the vertical phase fronts. Wind effects are more important for slower waves. In a windy background atmosphere it is the intrinsic direction of propagation (i.e., with respect to the moving atmosphere) that would be inferred by consideration of the anisotropy in airglow fluctuation brightness. These effects will be considered in a future study.

We have not considered the fact that in order to perform a single measurement an instrument requires a certain finite integration time to achieve a desired signal to noise ratio. The integration process will produce smearing, washing out the smaller scale waves in space-based airglow observations. Typically, integration times of several seconds are required, which will smear waves having horizontal wavelengths of ~50 km or less. This estimate is based on a 2.5 second integration time, the requirement of at least two such measurements to resolve the wave, and assuming a satellite speed of about 8 km/s. The simulations of *Brown and Hickey* [2000] show that when smearing effects are taken into account, wave direction can still be determined for the vast majority of waves of measurable amplitude in the airglow region.

Finally, we have assumed that the satellite motion occurs in a plane perpendicular to the horizontal phase fronts of the waves, which maximizes the difference between $B'/\bar{B}$ derived from forward and backward viewing. As the angle (θ) between the plane of the satellite motion and the phase fronts varies from $\pi/2$ to 0, these differences will approach zero. For $\theta = 0$ or π, the determination of propagation direction as proposed here is no longer possible. However, the orientation of the satellite velocity vector with respect to the wave vector would ordinarily be known (to within the π ambiguity), because other instruments, such as downward viewing 2-D imagers, could reveal the orientation of the phase fronts. Therefore, the limitations associated with our proposed method, as discussed above, would usually be assessable.

5. Conclusion

We have presented the results of simulations that show for atmospheric gravity waves having short vertical wavelengths the perturbation VER is generally asymmetric with respect to viewing direction, producing an observational difference for satellites viewing gravity wave perturbations in airglow emissions in the forward and backward viewing directions. These results imply that brightness fluctuations that are observed for the optically thick 0-0 band emission would always appear stronger for waves traveling towards the observer (satellite). For some smaller scale gravity waves, which are not expected to remain correlated over large horizontal distances, information useful for the interpretation of propagation direction could also be obtained using the optically thin 0-1 band emission. We have argued that for some waves brightness fluctuation differences between the forward and backward viewing directions should be observable and could be used to remove the 180° ambiguity in propagation direction for the waves. This will be a valuable tool for studying gravity waves from space because it is a method that does not rely on the simultaneous observations of the waves using ground-based instruments. Although we have considered both the optically thick (0-0) and optically thin (0-1) bands of the O_2A emission, our results show that the 0-0 band is better for resolving the 180° ambiguity in gravity wave propagation direction.

Acknowledgments. The authors are pleased to acknowledge support of this research by NASA grant NAGW-4762 to Clemson University. The comments of the two referees are gratefully acknowledged.

6. References

Brown, J. S., and M. P. Hickey, Gravity wave propagation directions inferred from satellite observations including smearing effects, *J. Geophys. Res., submitted*, 2000.

Francis, S. H., Propagation of internal acoustic-gravity waves around a spherical Earth, *J. Geophys. Res., 77*, 4221, 1972.

Fritts, D. C., R. C. Blanchard, and L. Coy, Gravity wave structure between 60 and 90 km inferred from Space Shuttle reentry data, *J. Atmos. Sci., 46*, 423-434, 1989.

Hedin, A. E., Extension of the MSIS thermosphere model into the middle and lower atmosphere, *J. Geophys. Res., 96*, 1159-1172, 1991.

Hickey, M. P., and R. L. Walterscheid, A Note on Gravity Wave-Driven Volume Emission Rate Weighted Temperature Perturbations Inferred from O_2 Atmospheric and O I 5577 Airglow Observations, *J. Geophys. Res., 104*, 4279, 1999.

Hickey, M. P., et al., Numerical Simulations of Gravity Waves Imaged over Arecibo during the 10-day January 1993 Campaign, *J. Geophys. Res., 102*, 11,475, 1997a.

Hickey, M. P., P. G. Richards, R. L. Walterscheid, and M. Wellman, Time-dependent, non-linear modeling of gravity wave-driven fluctuations in the O(^1S) nightglow, *EOS Trans. AGU, 78*, no.46, F510, 1997b.

Hickey, M. P., M. J. Taylor, C. S. Gardner, and C. R. Gibbons, Full-wave Modeling of Small-Scale Gravity Waves Using Airborne Lidar and Observations of the Hawaiian Airglow (ALOHA-93) O(^{1}S) Images and Coincident Na wind/temperature Lidar Measurements, *J. Geophys. Res., 103*, 6439, 1998.

Orlanski, I., and K. Bryan, Formation of the thermocline step structure by large-amplitude internal gravity waves, *J. Geophys. Res., 74*, 6975, 1969.

Schubert, G., R. L. Walterscheid, M. P. Hickey, and C. A. Tepley, Theory and Observations of Gravity Wave Induced Fluctuations in the OI (557.7 nm) Airglow, *J. Geophys. Res., 104*, 14,915-14,924, 1999.

Wallace, L., and D. M. Hunten, Dayglow of the oxygen A band, *J. Geophys. Res., 73*, 4813, 1968.

J. S. Brown and M. P. Hickey, Department of Physics and Astronomy, Clemson University, Clemson, SC 29634-0978. (e-mail: hickey@hubcap.clemson.edu)

(Received December 14, 1999; revised May 26, 2000; accepted July 28, 2000.)